



Robust Blind Watermarking Method for High Capacity RGB Image in Wavelet Domain

Salah Al-Obaidi¹, Natiq M. Abdali^{2*}, Hiba Al-Khafaji³

¹ Department of Computer Science, College of Science for Women, University of Babylon, Babel 51001, Iraq

² College of Arts, University of Babylon, Babel 51001, Iraq

³ Department of Software, College of Information Technology, University of Babylon, Babel 51001, Iraq

Corresponding Author Email: art.natiq.mutashar@uobabylon.edu.iq

Copyright: ©2025 The authors. This article is published by IETA and is licensed under the CC BY 4.0 license (<http://creativecommons.org/licenses/by/4.0/>).

<https://doi.org/10.18280/isi.300509>

ABSTRACT

Received: 7 March 2025

Revised: 17 May 2025

Accepted: 26 May 2025

Available online: 31 May 2025

Keywords:

color watermarking, invisibility, robustness, watermarking capacity, RGB images

Image watermarking is a tool to maintain the authentication and copyright protection of digital documents. RGB image is one of the media that is extensively distributed and transferred by the cloud. This type of digital data can be protected by hiding watermark protection logos. Furthermore, this type of images presents a media that can be used to hide more than one watermark. In this paper, a novel RGB image watermarking method based on DWT is used to embed three watermark logos, instead of one watermark logo. In each color channel, a watermark logo is embedded to increase the authentication criteria and capacity payload. To improve the robustness and invisibility, the wavelet transform is exploited to hide the watermark data in low-frequency bands rather than the pixel values. The proposed method is evaluated using three metrics, PSNR, NCC, and HD. The robustness of the proposed method is tested under various attack types, such as the noise, filter, and sharpening attacks. The experimental results show that the proposed RGB watermarking method has a good trade-off between robustness and invisibility and resistance to several attacks in the watermarked image. The method has been evaluated against various attacks (e.g., noise, filtering, compression, sharpening), demonstrating strong robustness while maintaining high image quality and achieving PSNR values between 37.8 and 51.2 dB. The proposed scheme outperforms several existing DWT-based RGB watermarking methods, showing a better trade-off between robustness, imperceptibility, and watermark capacity.

1. INTRODUCTION

Multimedia content has been increasingly distributed on the Internet and is now easily available to view and download [1]. However, this widespread availability of digital information raises the issue of protecting this digital content. Digital watermarking has emerged as a powerful technique that has emerged to address the issue of digital content protection by embedding identification or proprietary marks directly into the digital host, such as images, audio, and video. This protection technique is used for authentication, copyright, secret communication, biomedical data authentication, and many others [2-4]. Watermarking embeds the secret data, i.e., watermark, into the digital content of multimedia directly using embedding algorithms instead of making the multimedia content unintelligible/readable. In addition, the watermark can be visible or invisible, depending on the application [5]. However, in digital image watermarking, two of the most important principles, i.e. imperceptibility and robustness, are given priority in such an application [6]. The watermark that is hidden within the content should ideally remain undetectable by humans, ensuring it does not compromise the quality or disrupt the experience of the original material. At the same time, it needs to be strong enough to withstand typical signal processing actions without being compromised.

RGB image is one of the digital content that has been widely used in watermarking. The watermarking of RGB images plays a vital role in the protection of digital visual content by embedding imperceptible but resilient information within the red, green, and blue channels of an image. Unlike grayscale watermarks, RGB watermarks embed information in multiple color channels, enhancing robustness against attacks such as compression, crop ping, and noise addition [7]. Furthermore, color images can significantly increase the capacity and comprehension of information [8]. Therefore, RGB image watermarking plays a significant role in fields such as medical imaging, e-Commerce, and digital forensics, where data integrity and source identification are paramount. However, working on RGB space poses several significant challenges that impact its effectiveness and reliability. One primary challenge is achieving the balance between imperceptibility and robustness, which is inherently difficult. Another issue is the vulnerability to desynchronization attacks, where modifications, such as cropping or rotation, can interfere with the alignment between the embedded watermark and the detection algorithm, leading to failed watermark retrieval [9]. Furthermore, the growing adoption of deep learning techniques presents challenges such as the requirement for large training datasets and the potential risk of overfitting, which can affect the generalizability of watermarking models [10].

These challenges require ongoing research to develop more sophisticated and resilient watermarking methods that can effectively protect digital images while maintaining their quality. Digitally, several domain-based watermarking methods have been presented in both spatial and frequency domains. In the spatial domain, the watermarks are embedded in the pixels directly by modifying the values of intensities. One of the most popular methods for embedding watermarks in the spatial domain is least significant bit (LSB), which slightly affects the perceptibility of the image [11]. Quantization-based methods have also been used in this domain [12]. Despite the simplicity and low computation rate of applying the watermark in the spatial domain, the watermarking performed in the spatial domain is relatively weak against image-processing-based attacks, such as JPEG compression, filtering, and noise addition [5, 13, 14].

In the frequency (spectral) domain, various transforms have been experienced in watermarking applications to embed the watermark. In these transforms, the carrier image is firstly transformed into their frequency-based version and information hiding is carried out in the frequency components instead of the spatial content. The frequency domain based watermarking algorithms have the advantages of robustness against image processing based attack [13] and producing a watermarked image with less distortion [14]. The frequency domain digital watermarking can be achieved using the most common transforms such as discrete wavelet transform (DWT), Discrete Cosine Transformation (DCT), Discrete Fourier Transformation (DFT). These transforms offer greater robustness against various attacks [15]. DFT is the early transform that is explored to hide the watermark in image. In this context, we found the examples in studies [16-19]. DWT is also extensively used to meet the authentication copyright protection criteria in applications for protecting multimedia content. In DWT, the host image is decomposed into levels producing details and approximation sub-bands. DWT is commonly applied to embed a single watermark in one of the produced bands [20], however, two bands are also used to embed two watermarks [21]. Using these sub-bands for embedding provides better imperceptibility and quality of watermarked images. Consequently, the number of embedded watermarks can be increased without affecting the quality of images. In the proposed method, RGB carrier image is decomposed into two and three levels for each color band using DWT. Then, a single watermark is inserted in a low-level sub-band of each color band based on measuring the homogeneity of the region of embedding. This method provides better imperceptibility, quality of watermarked image, high-capacity watermark, and high authentication standard. The main contributions of the proposed method are:

1. Proposing a new blind RGB image watermarking method using DWT, embedding three watermark logos instead of just one. Each RGB channel contains a separate watermark, increasing authentication reliability and watermark capacity.
2. Enhancing the imperceptibility and robustness of the watermarking against various attacks by embedding the watermarks in the frequency domain instead of directly modifying pixel values. This scheme provides an additional layer of protection, leading to better invisibility and higher resistance to attacks like noise addition, filtering, and sharpening.
3. Utilizes all three RGB color channels for embedding multiple logos, significantly increasing payload capacity

without degrading the quality of the watermarked host image.

4. Blind extraction of the watermark without requiring the original image, making it more practical for real-world applications.

The remainder of this paper is structured as follows: Section 2 discusses the related studies on DWT based watermarking techniques. Section 3 explains the proposed watermarking method. The results are analyzed and discussed in Section 4. Finally, conclusions are drawn in Section 5.

2. RELATED WORK

Exploring the frequency domain to hide information contributes strongly to increase the security by including the frequency domain as an additional layer of protection. Therefore, many techniques of frequency domains are explored in watermarking to transform the host image to the frequency domain. However, this embedding in the frequency domain leads to extra distortions in the spatial domain [9]. The existing work on frequency domain based image watermarking is mainly based on using three most popular domains, i.e. DCT, DFT, and DWT. In this review, we will focus on the current work in the DWT domain.

2.1 Discrete wavelet transform

DWT based watermarking is widely used techniques that effectively and distinctively contributed to the watermarking techniques to improve the requirements of robustness and security, particularly in-blind and semi-blind applications [22]. Unlike DCT, the impact of the watermark on DWT coefficients is distributed across the entire image, thus meeting the criterion of being unnoticeable. One notable method that capitalizes on this characteristic involves embedding the watermark into the LL sub-band of DWT coefficients [23]. However, their method is non-blind and requires the original host image for watermark extraction, making it less resilient to certain types of attacks. A blind dual watermarking algorithm was proposed for digital color image authentication and copyright protection [24]. This approach applies DWT in the YCbCr color space for copyright protection while implementing authentication criteria in RGB color space through least significant bit (LSB) replacement. Despite being blind, this approach struggles with geometric robustness. DWT has also been applied to the Y component of the YCbCr color space to obtain non-overlapping sub-bands [25]. This approach used alpha blending to select high-entropy blocks for watermark embedding, achieving high imperceptibility and robustness. However, the method remained non-blind and unsuitable for real-time applications. Further refinement of this approach integrates compressed sensing with DWT in YCbCr color space [20]. By applying DWT exclusively to the Y channel and embedding compressed watermark blocks into low-frequency components, improved imperceptibility and robustness against various attacks were achieved.

Blind DWT-based color image watermarking have also evolved with innovative models. A blind watermarking scheme combining DWT and DCT has been developed for copyright protection and privacy preservation in RGB images [26]. This technique selects either the green or blue channel, partitions it into 4×4 blocks, applies DCT followed by two-level DWT on DC coefficients, and embeds the encrypted watermark into the LH sub-band of DWT to balance

imperceptibility and security. An advanced approach integrating DWT with Arnold transform and QR factorization has been proposed to enhance watermarked image invisibility and watermark robustness [27]. The method decomposes the host image using one-level DWT, encodes the watermark via Arnold transform, and employs QR decomposition to select optimal embedding locations.

Other transforms are also explored in color image watermarking [28]. The combinations of DCT, DFT, DWT and SVD have been explored by researchers and documented in various studies [29-35]. This class of hybrid methods has emerged to provide the most powerful watermarking models and improved the robustness. Nevertheless, integrating several transformations within a single technique leads to higher computational demands.

3. THE PROPOSED METHOD

This section introduces a robust blind watermarking technique utilizing the DFT domain instead of the spatial domain. Figure 1 shows the pipeline of the proposed method. This technique offers a robust watermarking approach that reduces the distortion and increases the imperceptibility. The proposed method examines the correlation among the frequencies of the adjacent pixels to estimate their smoothness or contrast levels, thereby determining the payload capacity for each embedding location. Accordingly, the blocks located in the edge area embed more data than those in the smooth area. In addition, the data embedded within the watermarked image is retrieved without the need to reference the original image.

3.1 Watermark logo embedding

Given the host RGB image, I , with size $N \times N$ and the binary watermark logo image, w , with size $n \times n$. I is firstly decomposed into its R, G, and B color components. Then, l -levels DWT is applied to these components, separately, resulting in the low-frequency component, i.e. approximation, for each color channel. The approximation coefficients are selected to embed w . Suppose A_i represents the matrix of approximation coefficients of the color components i , where $i \in \{R, G, \text{ and } B\}$, after applying the l -levels DWT. A_i is firstly partitioned into square blocks of size 3×3 with 30% of overlapping to ensure that the embedding positions are neither altered nor involved in calculating the embedding payload. For each overlapping block, the logo data is then hidden in A_i bit by bit. During embedding, the bit e , where $e = 1, 2, \dots, n \times n$, of w is added to the scanned overlapped block. This implies that when the embedded bit is equal to 1, an additional bit is added to the magnitude of the centered location in A_i . In contrast, if the embedded bit is equal to 0, the average of the four surrounding coefficients replaces the original coefficient magnitude of the centered location at the current scanned overlapped block, as demonstrated in Eq. (1).

$$\hat{A}_i^c = \begin{cases} A_i^c + w(e) & \text{if } w(e) = 1 \\ \bar{A}_i & \text{if } w(e) = 0 \end{cases} \quad (1)$$

where, \hat{A}_i^c and A_i^c represent the watermarked approximation and the original approximation coefficients of the centered position c , respectively, at the current scanned overlapped block in A_i . \bar{A}_i is the average approximation coefficient of the current scanned overlapped block, which is computed using

the following formula:

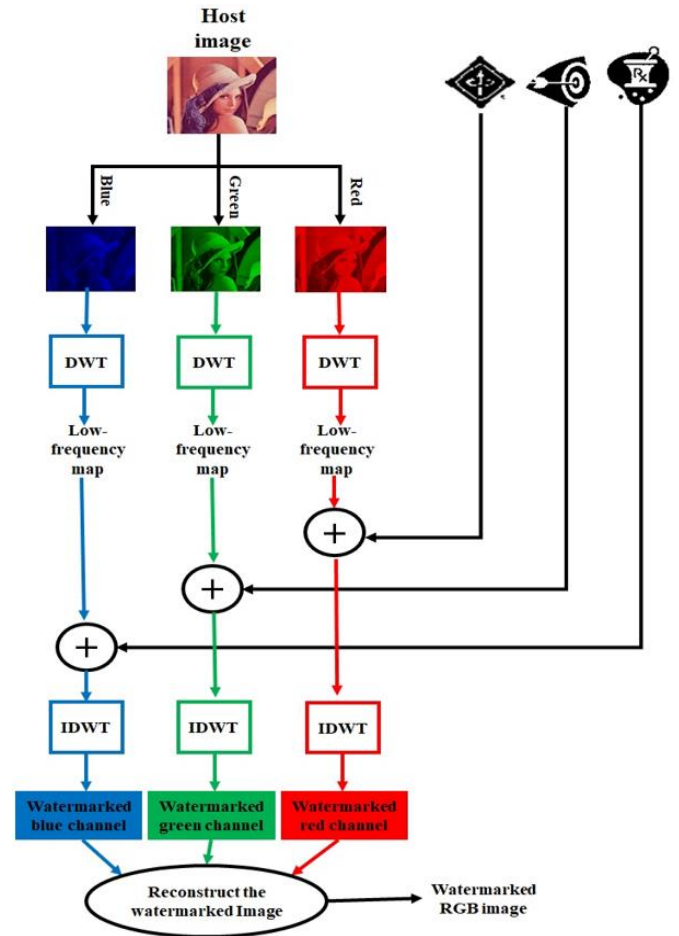


Figure 1. The block diagram of the proposed watermarking method

$$\bar{A}_i = \frac{A_i^l + A_i^r + A_i^b + A_i^u}{4} \quad (2)$$

where, A_i^l , A_i^r , A_i^b , and A_i^u represent the left, right, bottom, and upper neighboring of the current scanned location, respectively.

Applying Eq. (1) leads to increase or decrease the homogeneity in the target block, which contributes in the extraction stage without needing the origin host image. On one hand, the level of homogeneity inside each block is increased when the embedded bit is 0 by replacing A_i^c with \bar{A}_i . On the other hand, embedding a 1-bit secret decreases the homogeneity inside the target block. The aforementioned framework is repeated on each color channel, allowing the algorithm to hide three logo watermarks instead of a single watermark. Consequently, the payload increases by including three watermark logos, and the authentication is improved. After completion of the embedding task, the inverse discrete wavelet transform, IDWT, is applied to reconstruct the watermarked image \hat{I} .

Furthermore, making minimal changes using 2 leads to less noticeable and higher quality watermarking. In addition, utilizing the three color bands in hiding significantly increases the embedding capacity, allowing three watermarks to be embedded in a single image and enhancing the level of security. In the next section, blind extraction of the watermark logo images will be explained in detail.

3.2 Watermark logo extraction

The proposed extraction stage is blind where the embedded logo image is achieved without relying on the original carrier image or any information that can help as a reference. In this context, the same kernel that was used in embedding is used again to recover the watermark logos from the watermarked image.

Given the RGB watermarked image, \hat{I} , the watermarked color components R, G and B are obtained. Each color component is decomposed, separately, with l -levels DWT, resulting in the approximation and detail coefficients of this component. Suppose \hat{A}_i represents the matrix of approximation coefficients that includes a watermark logo of the color components i , where $i \in \{R, G, \text{ and } B\}$, after performing l -levels of DWT to \hat{I} . Then, \hat{A}_i is partitioned into overlapped blocks with 30% overlapping and it is scanned in a raster mode. At the current scanned overlapped block, a window mask, e.g. the kernel shown in Figure 2, is applied to extract the logo data as follows

$$\mathcal{D} = \left| \frac{\hat{A}_i^u + \hat{A}_i^r + \hat{A}_i^b + \hat{A}_i^l}{4} - \hat{A}_i^c \right| \quad (3)$$

where, \mathcal{D} represents the absolute value of the difference between the approximation coefficient at the center of current block, \hat{A}_i^c , and its neighboring. Then, logo image bits, \hat{w} , are collected as follows

0	1/4	0
1/4	-1	1/4
0	1/4	0

Figure 2. The cross operator of getting the approximation coefficient and its neighbors

The kernel structure shown in Figure 2 enables the algorithm to extract the logo bits without requiring knowledge of the embedding locations. This means that the embedding approach is blind. Then, logo image bits, \hat{w} , are collected as follows

$$\hat{w}(e) = \begin{cases} 0 & \text{if } \mathcal{D} \leq \tau \\ 1 & \text{otherwise,} \end{cases} \quad (4)$$

Eq. (4) implies that a watermark logo bit of 0 is extracted when the coefficients of the current block are homogeneous according to a predefined threshold τ . In contrast, a watermarked logo bit of 1 is obtained when the coefficients of the current block vary with the surrounding coefficients, less homogeneity. The level of homogeneity inside each block was already changed, increased or decreased, during the embedding phase. Therefore, this indicator of homogeneity level is used to extract the embedded data, making the extraction is blind. The value of τ is chosen between 0 and 1 to examine the degree of change in the homogeneity of the region being analyzed. Consequently, when the value of \mathcal{D} exceeds τ , this difference indicates that there is a change has been made in this region, which can be utilized to extract a bit with a value of 1; otherwise, a bit with a value of 0 is

extracted. The idea behind using a weight value of -1 in the center location of the kernel is to measure the disparity between the center point and the neighboring points by giving more importance to the center point where the logo data is assumed to be included. The coefficient values in the kernel in Figure 2 sum to zero, so they would give a response of zero in areas that contain a magnitude similar to its neighbors, which means a 0 bit of logo image. Otherwise, a 1 bit logo image is obtained.

The calculation of \mathcal{D} using the kernel in Figure 2 is a linear operation and is implemented using convolution. This means that the extraction stage using the proposed kernel operators is a lightweight process since the computational burden is linear.

4. EXPERIMENTAL RESULTS AND PERFORMANCE EVALUATION

In this section, the evaluation of the proposed method is presented in terms of its imperceptibility, robustness, and capacity. Several experiments were conducted to analyze the invisibility and robustness of the watermarking method proposed in this paper. The experiments utilized decomposition wavelet levels of two and three to assess how different analysis depths affect both imperceptibility and embedding capacity. To prevent edge artifacts during wavelet decomposition, the boundary handling mode is set to symmetric. The proposed method tested several mother wavelets and the reverse biorthogonal wavelet delivered the best performance in most scenarios. Figures 3 and 4 show RGB host and binary watermark images for the experiments where each host image is $512 \times 512 \times 3$, and the watermark logo image size is 32×32 . All experiments were carried out on a laptop with an Intel core i7-9750H 2.6GHz CPU with 16GB of RAM, using the MATLAB R2020a version.

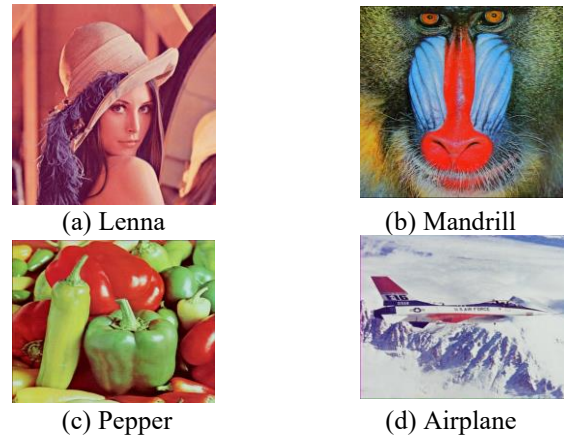


Figure 3. The set of cover images

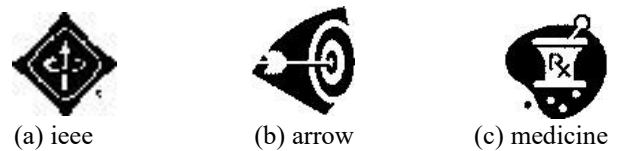


Figure 4. The set of watermark logo images

The experiments rely on 2 and 3-levels of DWT decomposition to get the approximation bands of color channels of the RGB image that is used to embed three watermark logos.

4.1 Evaluation metrics

The proposed watermarking method is evaluated using Peak Signal to Noise Ratio (PSNR), Hamming distance (HD), and normalized cross-correlation (NCC). PSNR is used to evaluate the imperceptibility of the watermarked host image as follows.

$$PSNR = 10 \times \log_{10} \frac{G^2}{\frac{1}{M \times N} \sum_{i=0}^M \sum_{j=0}^N (I_{ij} - I'_{ij})^2} \quad (5)$$

where, G is the maximum gray level found in the original host image. To evaluate the similarity between the original watermark logo image and the extracted watermark logo image, HD and NCC metrics are used. NCC is computed using the equation below.

$$NCC = \frac{\sum_{i=0}^m \sum_{j=0}^n (w_{ij} \times \hat{w}_{ij})}{\sqrt{\sum_{i=0}^m \sum_{j=0}^n (w_{ij})^2} \sqrt{\sum_{i=0}^m \sum_{j=0}^n (\hat{w}_{ij})^2}} \quad (6)$$

where, w and \hat{w} are the original watermark and the extracted watermark, respectively.

The number of concealed watermarks serves as an indicator of the capacity offered by the proposed method to store the authentication data.

HD is another metric used to evaluate the similarity between the original watermark logo image and the extracted watermark logo image. HD computation is given as Eq. (7).

$$HD = \sum_{i=0}^m \sum_{j=0}^n |w_{ij} - \hat{w}_{ij}| \quad (7)$$

4.2 Experimental results

Experiments were conducted to test the watermarking proposed scheme's visual quality, invisibility, robustness, and capacity. Invisibility is the ability to hide a watermark without affecting image quality. Tables 1 and 2 display experimental results in regards to image quality without any attack using 2 and 3-levels DWT. PSNR clearly shows that the method maintains consistent image quality. PSNR values of watermarked images after embedding three watermark logos achieved PSNR between 37.8 and 51.2 dB, demonstrating the excellent imperceptibility of the proposed method. HD and NCC values were used to evaluate the quality of the extracted watermark logos. HD and NCC values are one or close to one which means high quality extracted watermark images.


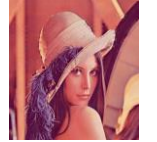






Table 1. PSNR, HD, and NCC results for watermarked images and extracted watermark logos of the proposed method without any attack using 2-levels of DWT

Host Images	PSNR	Logo Images	HD	NCC
Lenna	48.75	iecc	0.0107	0.9909
		arrow	0.0137	0.9882
		medicine	0.0010	0.9991
Mandrill	39.18	iecc	0.0010	0.9992
		arrow	0	1
		medicine	0	1
Pepper	44.30	iecc	0.0020	0.9984
		arrow	0.0020	0.9983
		medicine	0.0020	0.9981
Airplane	51.53	iecc	0.0020	0.9984
		arrow	0.0010	0.9992
		medicine	0.0010	0.9991

Table 2. PSNR, HD, and NCC results for watermarked images and extracted watermark logos of the proposed method without any attack using 3-levels of DWT

Host Images	PSNR	Logo Images	HD	NCC
Lenna	36.38	iecc	0.0010	0.9992
		arrow	0.0020	0.9983
		medicine	0	1
Mandrill	36.23	iecc	0	1
		arrow	0	1
		medicine	0	1
Pepper	34.90	iecc	0.0010	0.9992
		arrow	0.0010	0.9992
		medicine	0	1
Airplane	36.98	iecc	0	1
		arrow	0	1
		medicine	0	1

Table 3. The watermarked host images

Host Name	Watermarked Host Images	
	2-Levels DWT	3-Levels DWT
Lenna		
Mandrill		
Pepper		
Airplane		

Both HD and NCC values of the extracted watermark logos in Tables 1 and 2 indicate that the homogeneity within the scanned block, which was considered as a measure for extracting embedded data from the watermarked image in accordance with Eq. (3) and Eq. (4), yielded outstanding results. When the scanned block includes a high degree of homogeneity among the block's elements, 0 embedded bit is extracted. Conversely, 1 embedded bit is extracted where \hat{A}_i^c differs from its neighboring elements.

Table 3 shows the watermarked host images which have good visual quality. From the results of the evaluation metrics in Tables 1 and 2, we can observe a clear pattern: as PSNR values decrease, the HD and NCC values tend to improve, and vice versa. This pattern indicates a trade-off between imperceptibility and robustness. In accordance, when the imperceptibility goes down, robustness tends to increase. For example, Table 2 shows that using the Mandrill image as the host leads to fully extracting the embedded logos, i.e. high robustness, which affects image quality. Despite this trade-off, the algorithm achieved a good balance between imperceptibility and robustness in some cases. Notably, with the Airplane and Lenna images in Table 1, both high PSNR and strong HD/NCC scores were achieved. The Airplane host image, for instance, has a PSNR of 51.53, while the NCC

values for the extracted logos range from 0.9984 and 0.9992. Furthermore, the high resolution extracted logos displayed in Table 4 demonstrate that these logos are either fully or almost fully extracted. These results highlight the influence of considering homogeneity within each scanned block on both producing the watermarked image and collecting the logo's data.

Table 4. Extracted watermark logo images

Host's Name	Logo's Name	2-Levels DWT	3-Levels DWT
Lenna	ieee		
	arrow		
	medicine		
Mandrill	ieee		
	arrow		
	medicine		
Pepper	ieee		
	arrow		
	medicine		
Airplane	ieee		
	arrow		
	medicine		

4.3 Robustness evaluation

The above experiments demonstrate that the proposed scheme produces significant results on several RGB images. The robustness of the proposed method is assessed against various noise, filtering, and other attacks. These attacks include salt & pepper noise, Gaussian noise, speckle noise, sharpening, median filter, average filter, Gaussian low pass, and motion blur. In addition, various geometric attacks, such as rotation, scaling, and cropping, and image processing attacks, such as histogram equalization and contrast adjustment, are also employed. After applying a specific attack,

the watermark is recovered and the similarity metrics, NCC and HD, of the extracted watermark are computed to evaluate the resistance of the watermarked image produced by the proposed method in relation to an attack. Tables 5 and 6 show the results of applying several attacks on the watermarked images in terms of HD and NCC using wavelet decomposition of 2 and 3 levels, respectively.

The results of HD and NCC in Table 5 demonstrate that the proposed method produces a robust watermarked image that can resist most attacks and presents high quality extracted watermark logos. Furthermore, the proposed method introduced a significant robustness against Gaussian and median filters. This exceptional performance demonstrates that those types of attacks have minimal impact on the quality of the carrier. Median filter leads to increase the smoothness; i.e. homogeneity, of an image, which means that the data of object inside the logo are either fully or partially extracted since these extracted data are collected from homogeneous blocks. Additionally, it has also demonstrated strong robustness against speckle noise and sharpening attacks. Moreover, the algorithm proved to be quite robust against image processing attacks, such as sharpening and contrast adjustment as shown in Table 5. Notably, the watermarked images show maintained high resistance to contrast adjustment, achieving an NCC of up to 0.9934. The algorithm also performed well with cropping attack by showing a strong NCC and HD compared to other types of geometric distortions. The same performance has also been achieved in Table 6, especially for median filter with 3×3 kernel size.

4.4 Comparison with existing methods

The proposed method is compared with existing methods on DWT-based watermarking. PSNR is used to compare the proposed method with the current work according to invisibility. Table 7 shows the PSNR results of the proposed method and the existing work for RGB image watermarking.

In Table 7, the proposed method resulted in high PSNR values for certain images, even though three watermark logos were embedded instead of only one. This superior performance is due to the fact that the embedding is done in the frequency domain rather than in the spatial domain. Therefore, inserting the watermark data within the frequencies has less impact on image quality compared to modifying the pixel values. Furthermore, considering the homogeneity among neighboring coefficients contributes positively during the embedding stage.

Table 5. Values of HD and NCC for different attacks using 2-levels wavelet decomposition

Name of Attack	Name of Logos	Lenna		Mandrill		Pepper		Airplane	
		HD	NCC	HD	NCC	HD	NCC	HD	NCC
No attack	ieee	0.0088	0.9925	0	1	0.0013	0.9989	0.0006	0.9995
	arrow	0.0094	0.9920	0	1	0.0019	0.9984	0.0013	0.9989
	medicine	0.0031	0.9977	0	1	0.0037	0.9973	0.0044	0.9968
Salt&Pepper noise	ieee	0.0674	0.9432	0.0264	0.9784	0.0508	0.9584	0.0430	0.9693
	arrow	0.0635	0.9446	0.0391	0.9677	0.0586	0.9508	0.0586	0.9506
var=0.001	medicine	0.0654	0.9384	0.0439	0.9597	0.0566	0.9464	0.0635	0.9384
Gaussian noise	ieee	0.0127	0.9893	0.0020	0.9984	0.0039	0.9967	0.0088	0.9926
	arrow	0.0078	0.9933	0	1	0.0059	0.9950	0.0039	0.9966
var=0.003	medicine	0.0166	0.9840	0.0039	0.9963	0.0059	0.9944	0.0146	0.9859
Speckle noise	ieee	0.0693	0.9400	0.0117	0.9901	0.0439	0.9624	0.0439	0.9624
	arrow	0.0840	0.9252	0.0068	0.9941	0.0352	0.9694	0.0498	0.9563
	medicine	0.0596	0.9412	0.0156	0.9849	0.0303	0.9705	0.0742	0.9261
Median 3×3	ieee	0.0029	0.9975	0.0010	0.9992	0.0029	0.9975	0.0020	0.9984
	arrow	0	1	0	1	0.0029	0.9975	0	1

Median 5×5	medicine	0.0020	0.9981	0.0020	0.9981	0.0029	0.9972	0.0020	0.9981
	ieee	0.0029	0.9975	0.0010	0.9992	0.0029	0.9975	0.0020	0.9984
	arrow	0	1	0	1	0.0039	0.9966	0	1
Average 3×3	medicine	0.0020	0.9981	0.0020	0.9981	0.0029	0.9972	0.0020	0.9981
	ieee	0.1992	0.8388	0.3555	0.7870	0.2979	0.7956	0.2930	0.7875
	arrow	0.2930	0.7740	0.3809	0.7700	0.3379	0.7716	0.2383	0.8205
Motion blur	medicine	0.2793	0.7621	0.4014	0.7394	0.4082	0.7066	0.2363	0.7852
	ieee	0.1768	0.8501	0.3320	0.7961	0.2354	0.8251	0.1973	0.8459
	arrow	0.2500	0.7949	0.3428	0.7842	0.2998	0.7872	0.1719	0.8627
Gaussian low pass	medicine	0.2178	0.7966	0.3418	0.7639	0.3574	0.7284	0.1582	0.8435
	ieee	0.2168	0.8391	0.3750	0.7799	0.3262	0.7908	0.3193	0.7897
	arrow	0.3145	0.7789	0.3936	0.7680	0.3584	0.7703	0.2773	0.8077
Sharpening	medicine	0.2168	0.8595	0.2441	0.8612	0.2607	0.8429	0.1650	0.8898
	ieee	0.0547	0.9531	0.0146	0.9877	0.0498	0.9574	0.0313	0.9735
	arrow	0.0645	0.9434	0.0645	0.9434	0.0498	0.9564	0.0215	0.9815
Contrast adjustment	medicine	0.0771	0.9241	0.0264	0.9746	0.0645	0.9364	0.0469	0.9542
	ieee	0.0166	0.9860	0.0889	0.9326	0.0156	0.9871	0.0078	0.9934
	arrow	0.0430	0.9633	0.2168	0.8534	0.0264	0.9776	0.0127	0.9891
Histogram equalization	medicine	0.0313	0.9708	0.0908	0.9224	0.0215	0.9795	0.0078	0.9925
	ieee	0.2158	0.8199	0.3652	0.7686	0.3398	0.7712	0.4160	0.7103
	arrow	0.3838	0.7644	0.3984	0.7710	0.3994	0.7670	0.4063	0.7658
Scaling factor= 0.5	medicine	0.4385	0.7237	0.4707	0.7230	0.4688	0.7173	0.4707	0.9198
	ieee	0.2061	0.8313	0.3672	0.7816	0.3018	0.7936	0.3018	0.7892
	arrow	0.3125	0.7639	0.3926	0.7657	0.3467	0.7665	0.2617	0.8031
Rotation 1800	medicine	0.2861	0.7564	0.4258	0.7281	0.4102	0.7103	0.2373	0.7819
	ieee	0.4053	0.7709	0.4043	0.7718	0.4053	0.7709	0.4053	0.7709
	arrow	0.4141	0.7655	0.4141	0.7655	0.4141	0.7655	0.4141	0.7655
Cropping	medicine	0.4795	0.7211	0.4785	0.7211	0.4795	0.7211	0.4766	0.7228
	ieee	0.0820	0.9319	0.0820	0.9319	0.0820	0.9319	0.0820	0.9319
	arrow	0.0869	0.9278	0.0869	0.9278	0.0869	0.9278	0.0869	0.9278
	medicine	0.0957	0.9128	0.0957	0.9128	0.0957	0.9128	0.0957	0.9128

Table 6. Values of HD and NCC for different attacks using 3-levels wavelet decomposition

Name of Attack	Name of Logos	Lenna		Mandrill		Pepper		Airplane	
		HD	NCC	HD	NCC	HD	NCC	HD	NCC
No attack	ieee	0.0006	0.9995	0.0006	0.9995	0.0013	0.9989	0	1
	arrow	0.0013	0.9989	0	1	0.0006	0.9995	0	1
	medicine	0	1	1	1	0	1	0.0013	0.9991
Salt&Pepper noise	ieee	0.1006	0.9247	0.1328	0.9040	0.1094	0.9189	0.908	0.9315
	arrow	0.1094	0.9169	0.1172	0.9125	0.1377	0.8955	0.0879	0.9322
	medicine	0.0713	0.9543	0.0605	0.9611	0.0771	0.9512	0.0605	0.9611
Gaussian noise var=0.003	ieee	0.002	0.9984	0.0020	0.9984	0.0049	0.9959	0.0059	0.9951
	arrow	0.0078	0.9933	0	1	0.0029	0.9975	0.0059	0.9950
	medicine	0.0029	0.9972	0	1	0.0010	0.9991	0.0059	0.9944
Speckle noise var=0.003	ieee	0.0088	0.9926	0.0039	0.9967	0.0088	0.9926	0.0088	0.9926
	arrow	0.0195	0.9831	0.0010	0.9992	0.0107	0.9907	0.0088	0.9924
	medicine	0.0059	0.9944	0.0020	0.9981	0.0059	0.9944	0.0117	0.9887
Median 3×3	ieee	0.0010	0.9992	0	1	0.0010	0.9992	0	1
	arrow	0.0020	0.9983	0	1	0.0010	0.9992	0	1
	medicine	0	1	0	1	0	1	0	1
Median 5×5	ieee	0.0010	0.9992	0.001	0.9992	0.0020	0.9984	0.0010	0.9992
	arrow	0.0029	0.9975	0	1	0.0010	0.9992	0	1
	medicine	0	1	0	1	0	1	0	1
Average 3×3	ieee	0.2754	0.8188	0.3330	0.7938	0.2637	0.8288	0.1963	0.8613
	arrow	0.3447	0.7813	0.3418	0.7910	0.3496	0.7852	0.2539	0.8245
	medicine	0.3301	0.7642	0.3896	0.7492	0.3799	0.7516	0.2119	0.8301
Motion blur	ieee	0.2168	0.8459	0.2754	0.8222	0.2021	0.8609	0.0859	0.9319
	arrow	0.2783	0.8125	0.2871	0.8158	0.2969	0.8099	0.1650	0.8752
	medicine	0.2520	0.8056	0.3223	0.7788	0.3223	0.7783	0.1494	0.8710
Gaussian low pass	ieee	0.2783	0.8144	0.3203	0.799	0.2559	0.8323	0.1875	0.8667
	arrow	0.3398	0.7835	0.333	0.7944	0.3457	0.7874	0.2402	0.8317
	medicine	0.1924	0.8796	0.2031	0.8803	0.2207	0.8694	0.1641	0.8919
Sharpening	ieee	0.0313	0.9737	0.0166	0.986	0.0107	0.9910	0.0156	0.9868
	arrow	0.0264	0.9773	0.0029	0.9975	0.0137	0.9882	0.0244	0.9788
	medicine	0.0371	0.9641	0.0146	0.9861	0.0107	0.9897	0.0342	0.9669
Contrast adjustment	ieee	0.0508	0.9579	0.0449	0.9635	0.0967	0.9245	0.0615	0.9499
	arrow	0.1045	0.9148	0.1221	0.9085	0.0742	0.9385	0.0752	0.9379
	medicine	0.0869	0.9239	0.1055	0.9112	0.0664	0.9394	0.1045	0.9071

Histogram equalization	ieee	0.4014	0.7714	0.4033	0.7707	0.4004	0.7728	0.4023	0.7721
	arrow	0.4150	0.7619	0.4141	0.7634	0.4131	0.7643	0.4121	0.7657
	medicine	0.4775	0.7199	0.4658	0.7216	0.4795	0.7205	0.4775	0.7195
Scaling scaling factor= 0.5	ieee	0.2549	0.8271	0.3350	0.7953	0.2480	0.8358	0.1670	0.8794
	arrow	0.3252	0.7916	0.3535	0.7855	0.3330	0.7939	0.2227	0.8417
	medicine	0.3027	0.7773	0.3828	0.7576	0.3545	0.7663	0.1875	0.8447
Rotation 1800	ieee	0.4033	0.7722	0.4043	0.7718	0.4043	0.7718	0.4043	0.7718
	arrow	0.4141	0.7655	0.4141	0.7655	0.4141	0.7655	0.4141	0.7655
	medicine	0.4785	0.7221	0.4785	0.7221	0.4785	0.7221	0.4785	0.7221
Cropping	ieee	0.1621	0.8695	0.1611	0.8704	0.1611	0.8704	0.1611	0.8704
	arrow	0.1689	0.8577	0.1689	0.8577	0.1689	0.8577	0.1689	0.8577
	medicine	0.2422	0.7803	0.2422	0.7803	0.2422	0.7803	0.2422	0.7803

Table 7. Comparison the proposed method and the existing work on RGB image

Method	Watermarking Type	Embedding Capacity	Host Images			
			Lenna	Mandrill	Pepper	Airplane
Cheema et al. [8]	Simi-Blind	1	45.57	45.34	45.67	45.34
Ahmadi et al. [36]	Blind	1	53.14	49.12	51.98	50.48
Elbasi [22]	Non-blind	1	42.52	—	44.52	—
Vaidya and Mouli [20]	Blind	1	47.58	47.52	47.46	47.53
Proposed Method	Blind	3	48.75	39.18	44.30	51.53

5. CONCLUSIONS

In this paper, a novel RGB image watermarking method based on DWT is used to embed three watermark logos. The imperceptibility and robustness of the proposed method are analyzed experimentally and the results show that the watermarked host images have good visual quality and PSNR despite the increased payload capacity. In addition, the watermarks are clearly extracted from the watermarked host image under different attacks with the relatively high NCCs and HD. Moreover, the comparison with the related works show that the proposed method has a better performance in terms of robustness for most attacks. It is important to note that the proposed method demonstrates robust defense abilities against median filter, Gaussian noise, speckle noise, and sharpening attacks. The proposed watermarking method also shows strong performance against some image processing attacks, such as sharpening and contrast adjustment.

The proposed watermarking method performs well overall but has some limitations. It relies only on the DWT domain, showing weaker resistance to some geometric attacks like rotation and scaling, and uses a fixed-size embedding block, which may not be ideal for all image types. The overlapping block approach, although effective, adds extra computational overhead. The method lacks built-in security features like encryption. Future research could focus on extending the method to hybrid transform domains (e.g., DWT-DCT or DWT-SVD), optimizing the embedding and extraction processes using adaptive or learning-based techniques, enhancing robustness to geometric distortions, adapting the approach for specific application areas like medical imaging or cloud storage, incorporating cryptographic security, and improving computational efficiency for real-time or hardware-based implementations.

REFERENCES

[1] Hu, H.T. (2024). Synergistic compensation for RGB-based blind color image watermarking to withstand

JPEG compression. *Journal of Information Security and Applications*, 80: 103673. <https://doi.org/10.1016/j.jisa.2023.103673>

[2] Hadad, A.A.A., Khalid, H.N., Naser, Z.S., Taha, M.S. (2022). A robust color image watermarking scheme based on discrete wavelet transform domain and discrete slantlet transform technique. *Ingenierie des Systemes d'Information*, 27(2): 313. <https://doi.org/10.18280/isi.270215>

[3] Kunhoth, J., Subramanian, N., Al-Maadeed, S., Bouridane, A. (2023). Video steganography: Recent advances and challenges. *Multimedia Tools and Applications*, 82(27): 41943-41985. <https://doi.org/10.1007/s11042-023-14844-w>

[4] Sharma, N., Anand, A., Singh, A.K., Agrawal, A.K. (2023). Optimization based ECG watermarking in RDWT-SVD domain. *Multimedia Tools and Applications*, 82: 5031-5047. <https://doi.org/10.1007/s11042-021-11519-2>

[5] Asikuzzaman, M., Pickering, M.R. (2017). An overview of digital video watermarking. *IEEE Transactions on Circuits and Systems for Video Technology*, 28(9): 2131-2153. <https://doi.org/10.1109/TCSVT.2017.2712162>

[6] Mishra, A., Agarwal, C., Sharma, A., Bedi, P. (2014). Optimized gray-scale image watermarking using DWT-SVD and Firefly Algorithm. *Expert Systems with Applications*, 41(17): 7858-7867. <https://doi.org/10.1016/j.eswa.2014.06.011>

[7] Zhang, F., Luo, T., Jiang, G., Yu, M., Xu, H., Zhou, W. (2019). A novel robust color image watermarking method using RGB correlations. *Multimedia Tools and Applications*, 78: 20133-20155. <https://doi.org/10.1007/s11042-019-7326-9>

[8] Cheema, A.M., Adnan, S.M., Mehmood, Z. (2020). A novel optimized semi-blind scheme for color image watermarking. *IEEE Access*, 8: 169525-169547. <https://doi.org/10.1109/ACCESS.2020.3024181>

[9] Boujerfaoui, S., Riad, R., Douzi, H., Ros, F., Harba, R. (2022). Image watermarking between conventional and

- learning-based techniques: A literature review. *Electronics*, 12(1): 74. <https://doi.org/10.3390/electronics12010074>
- [10] Ben Jabra, S., Ben Farah, M. (2024). Deep learning-based watermarking techniques challenges: A review of current and future trends. *Circuits, Systems, and Signal Processing*, 43(7): 4339-4368. <https://doi.org/10.1007/s00034-024-02651-z>
- [11] Sharma, D., Saxena, R., Singh, N. (2017). Dual domain robust watermarking scheme using random DFRFT and least significant bit technique. *Multimedia Tools and Applications*, 76(3): 3921-3942. <https://doi.org/10.1007/s11042-016-4095-6>
- [12] Chou, C.H., Wu, T.L. (2003). Embedding color watermarks in color images. *EURASIP Journal on Advances in Signal Processing*, 2003: 1-9.
- [13] Mohanarathinam, A., Kamalraj, S., Prasanna Venkatesan, G.K.D., Ravi, R.V., Manikandababu, C.S. (2020). Digital watermarking techniques for image security: A review. *Journal of Ambient Intelligence and Humanized Computing*, 11(8): 3221-3229. <https://doi.org/10.1007/s12652-019-01500-1>
- [14] Su, Q., Liu, D., Yuan, Z., Wang, G., Zhang, X., Chen, B., Yao, T. (2019). New rapid and robust color image watermarking technique in spatial domain. *IEEE Access*, 7: 30398-30409. <https://doi.org/10.1109/ACCESS.2019.2895062>
- [15] Al-Na'amneh, Q., Almomani, A., Nasayreh, A., Nahar, K.M., Gharaibeh, H., Al Mamlook, R.E., Alauthman, M. (2024). Next generation image watermarking via combined DWT-SVD technique. In 2024 2nd International Conference on Cyber Resilience (ICCR), Dubai, United Arab Emirates, pp. 1-10. <https://doi.org/10.1109/ICCR61006.2024.10532782>
- [16] Lin, C.Y., Wu, M., Bloom, J.A., Cox, I.J., Miller, M.L. and Lui, Y.M. (2001). Rotation, scale, and translation resilient watermarking for images. *IEEE Transactions on Image Processing*, 10(5): 767-782.
- [17] Solachidis, V., Pitas, L. (2001). Circularly symmetric watermark embedding in 2-D DFT domain. *IEEE Transactions on Image Processing*, 10(11): 1741-1753. <https://doi.org/10.1109/83.967401>
- [18] Tang, C.W., Hang, H.M. (2003). A feature-based robust digital image watermarking scheme. *IEEE Transactions on Signal Processing*, 51(4): 950-959. <https://doi.org/10.1109/TSP.2003.809367>
- [19] Bao, B., Wang, Y. (2024). A robust blind color watermarking algorithm based on the Radon-DCT transform. *Multimedia Tools and Applications*, 83(24): 64663-64682. <https://doi.org/10.1007/s11042-023-17875-5>
- [20] Vaidya, S.P., Mouli, P.C. (2024). Robust digital color image watermarking based on compressive sensing and DWT. *Multimedia Tools and Applications*, 83(2): 3357-3371. <https://doi.org/10.1007/s11042-023-15349-2>
- [21] Kumar, C. (2024). Hybrid optimization for secure and robust digital image watermarking with DWT, DCT and SPIHT. *Multimedia Tools and Applications*, 83(11): 31911-31932. <https://doi.org/10.1007/s11042-023-16903-8>
- [22] Elbasi, E. (2022). A non-blind watermarking technique using flexible scaling factor in wavelet transform. In 2022 45th International Conference on Telecommunications and Signal Processing (TSP), Prague, Czech Republic, pp. 150-155. <https://doi.org/10.1109/TSP55681.2022.9851257>
- [23] Jane, O., Elbaşı, E. (2014). A new approach of nonblind watermarking methods based on DWT and SVD via LU decomposition. *Turkish Journal of Electrical Engineering and Computer Sciences*, 22(5): 1354-1366. <https://doi.org/10.3906/elk-1212-75>
- [24] Liu, X.L., Lin, C.C., Yuan, S.M. (2016). Blind dual watermarking for color images' authentication and copyright protection. *IEEE Transactions on Circuits and Systems for Video Technology*, 28(5): 1047-1055. <https://doi.org/10.1109/TCSVT.2016.2633878>
- [25] Kumar, S., Singh, B.K. (2021). DWT based color image watermarking using maximum entropy. *Multimedia Tools and Applications*, 80: 15487-15510. <https://doi.org/10.1007/s11042-020-10322-9>
- [26] Mohammed, A.O., Hussein, H.I., Mstafa, R.J., Abdulazeez, A.M. (2023). A blind and robust color image watermarking scheme based on DCT and DWT domains. *Multimedia Tools and Applications*, 82(21): 32855-32881. <https://doi.org/10.1007/s11042-023-14797-0>
- [27] Nha, P.T., Thanh, T.M. (2021). A combination of DWT and QR decomposition for color image watermarking. In 2021 13th International Conference on Knowledge and Systems Engineering (KSE), Bangkok, Thailand, pp. 1-6. <https://doi.org/10.1109/KSE53942.2021.9648714>
- [28] Kusnawi, K., Ipmawati, J., Prabowo, D.P. (2024). Enhancing quality measurement for visible and invisible watermarking based on M-SVD and DCT. *Bulletin of Electrical Engineering and Informatics*, 13(4): 2537-2546. <https://doi.org/10.11591/eei.v13i4.7884>
- [29] Lai, C.C., Tsai, C.C. (2010). Digital image watermarking using discrete wavelet transform and singular value decomposition. *IEEE Transactions on Instrumentation and Measurement*, 59(11): 3060-3063. <https://doi.org/10.1109/TIM.2010.2066770>
- [30] Kang, X.B., Zhao, F., Lin, G.F., Chen, Y.J. (2018). A novel hybrid of DCT and SVD in DWT domain for robust and invisible blind image watermarking with optimal embedding strength. *Multimedia Tools and Applications*, 77: 13197-13224. <https://doi.org/10.1007/s11042-017-4941-1>
- [31] Singh, O.P., Singh, K.N., Singh, A.K., Agrawal, A.K., Zhou, H. (2024). An improved robust algorithm for optimisation-based colour medical image watermarking. *Computers and Electrical Engineering*, 117: 109278. <https://doi.org/10.1016/j.compeleceng.2024.109278>
- [32] Hamidi, M., Haziti, M.E., Cherifi, H., Hassouni, M.E. (2018). Hybrid blind robust image watermarking technique based on DFT-DCT and Arnold transform. *Multimedia Tools and Applications*, 77: 27181-27214. <https://doi.org/10.1007/s11042-018-5913-9>
- [33] Devi, K.J., Singh, P., Bilal, M., Nayyar, A. (2024). Enabling secure image transmission in unmanned aerial vehicle using digital image watermarking with H-Grey optimization. *Expert Systems with Applications*, 236: 121190. <https://doi.org/10.1016/j.eswa.2023.121190>
- [34] Begum, M., Shorif, S. B., Uddin, M. S., Ferdush, J., Jan, T., Barros, A., Whaiduzzaman, M. (2024). Image watermarking using discrete wavelet transform and singular value decomposition for enhanced imperceptibility and robustness. *Algorithms*, 17(1): 32. <https://doi.org/10.3390/a17010032>

- [35] Al-Khafaji, H., Al-Himyari, B., Alharbi, H. (2024). Enhancing image watermarking: An innovative multi-objective genetic algorithm-based DWT-SVD approach for robustness and imperceptibility. *International Journal of Safety & Security Engineering*, 14(6): 1921. <https://doi.org/10.18280/ijssse.140626>
- [36] Ahmadi, S.B.B., Zhang, G., Rabbani, M., Boukela, L., Jelodar, H. (2021). An intelligent and blind dual color image watermarking for authentication and copyright protection. *Applied Intelligence*, 51: 1701-1732. <https://doi.org/10.1007/s10489-020-01903-0>